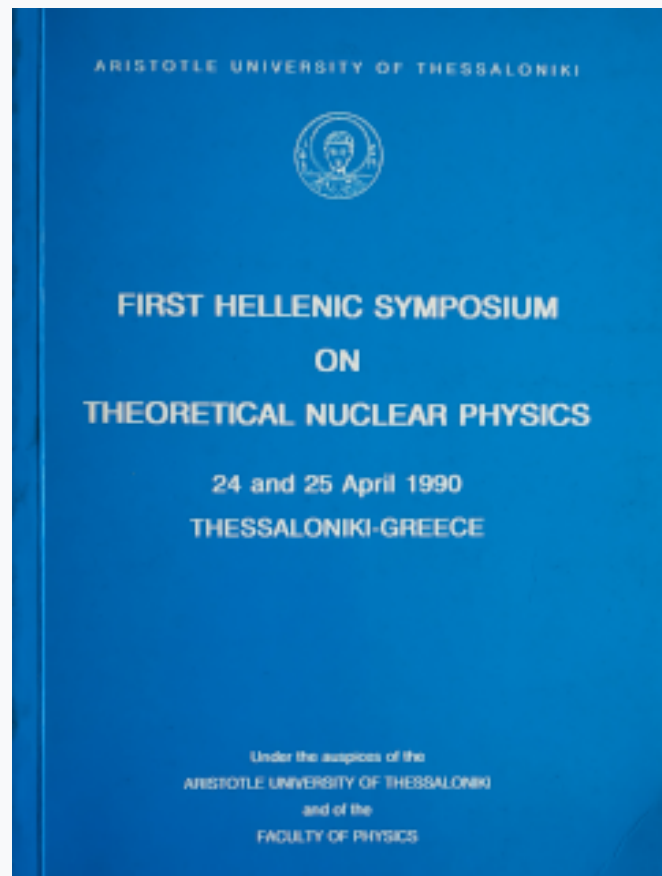


HNPS Advances in Nuclear Physics

Vol 1 (1990)

HNPS1990



Clusters in Atoms and Nuclei

G. S. Anagnostatos

doi: [10.12681/hnps.2829](https://doi.org/10.12681/hnps.2829)

To cite this article:

Anagnostatos, G. S. (2020). Clusters in Atoms and Nuclei. *HNPS Advances in Nuclear Physics*, 1, 98–114.
<https://doi.org/10.12681/hnps.2829>

Clusters in Atoms and Nuclei

G. S. Anagnostatos

Institute of Nuclear Physics

National Center for Scientific Research "Demokritos"

GR-153 10, Aghia Paraskevi-Attiki, GREECE

ABSTRACT: Small aggregates of particles, possessing different properties than those in bulk (i.e., in crystals or in nuclear matter), are reviewed here. Specifically, while some categories of atomic clusters (regular or bosonic) are in a solid state of matter and their structure possesses, more or less, definite geometric picture of packing of spheres standing for atoms, some other categories of atomic clusters (quantum or fermionic) are in a liquid (or gas) state of matter and their structure follows quantum mechanics whose only the average forms have a geometrical representation. These quantum clusters can be extended to include nucleon clusters of spheres standing for the nucleon bags with rather impressive results. All families of clusters considered together could be seen as a fifth state of matter.

1. INTRODUCTION

The physics of microclusters is a very rapidly growing, new area of science. It is an interdisciplinary topic and thus attracts scientists from many related sciences, e.g. solid state, chemistry, atomic physics, plasma physics, crystallography, and nuclear physics, both theorists and experimentalists. Their research takes place both in academic institutes and industries, since a large number of important applications are immediately expected, e.g., in catalysis.

An aggregate of atoms or molecules is called a microcluster when the number of the constituent particles does not, usually, exceed 1000. Their electronic properties are significantly different than the properties of the same material in bulk. One of the first ways for their production is via supersonic expansion of vapours of the material produced in an oven. After their production a mass spectrometer separates the different species according to their number of particles. Their state of matter can be solid, liquid, or gas.

One of the major properties of microclusters is the appearance of magic numbers, i.e., the property that microclusters possessing specific numbers of constituent particles exhibit exceptional properties in comparison to those of species with neighboring numbers of particles.

The theoretical investigation of such numbers follows two distinct paths. The one is based on the properties of the delocalized electrons in clusters (Knight et al, 1984), while the other on the equilibrium geometry of the constituent particles (Echt et al 1981, and Anagnostatos 1987). Different magic numbers appear for different groups of elements , e.g., alkali, noble gases, alkali halide and their mixtures, or even for the same group of elements under different conditions of preparation (e.g., born neutral or born ionized) and temperature or cluster size.

It is a very important fact that neutral alkali (Knight et al 1984) or alkali like (Ag, Au, Cu) clusters possess magic numbers very closely related to those in nuclear physics (e.g., 2, 8, 20, 40,...). This similarity does not seem incidental and is due to the common fermionic nature of nucleons and neutral alkali atoms (i.e., odd number of electrons; Anagnostatos 1991a and b), which is consistent with the liquid (or gas) state of matter valid for both alkali clusters and nuclei. This is further consistent with the fact that bosonic clusters (i.e., clusters with atoms possessing even number of electrons as in rare gases, for example) very closely resemble a solid state of matter.

The resemblance between alkali (or alkali like) quantum clusters and atomic nuclei gives a hint of an alternative approach of studying atomic nuclei.

2. ATOMIC CLUSTERS

Magic numbers in microclusters.

Some examples of mass spectra and related magic numbers are shown in Figures 1(a)-(d). Specifically, in Figure 1(a) the mass spectrum of xenon clusters is shown (Echt et al 1981), where the bold numbers over prominent peaks stand for the relevant magic numbers. In Figures 1(b)-(d)

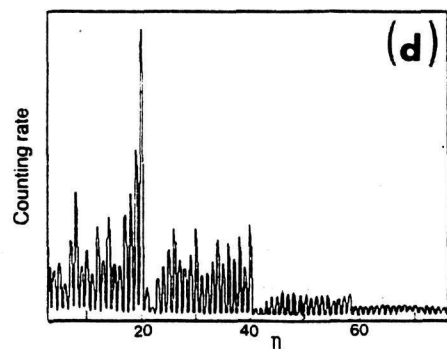
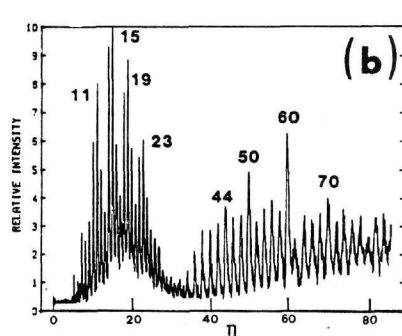
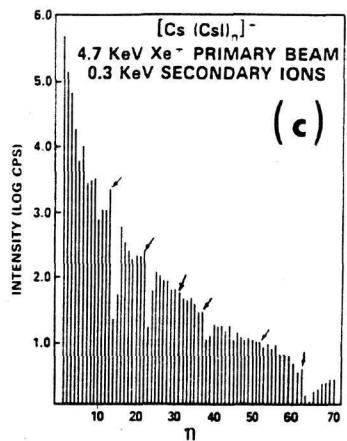
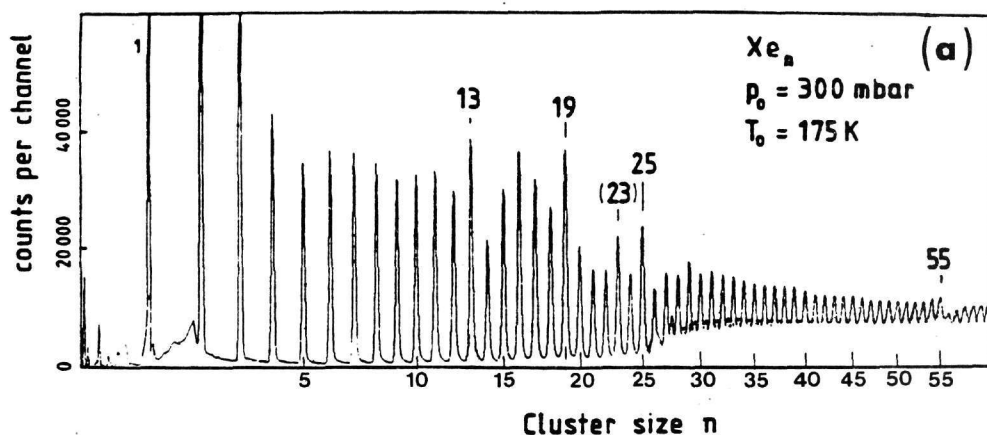


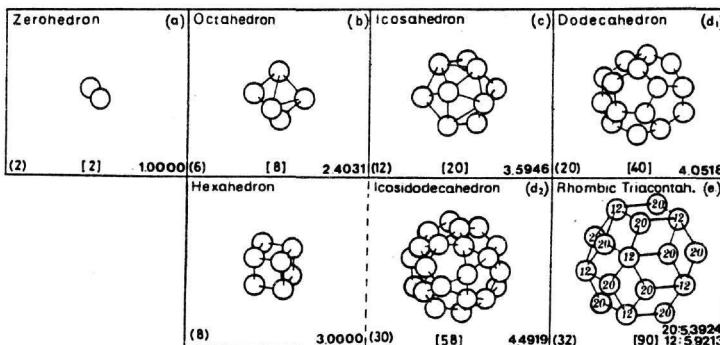
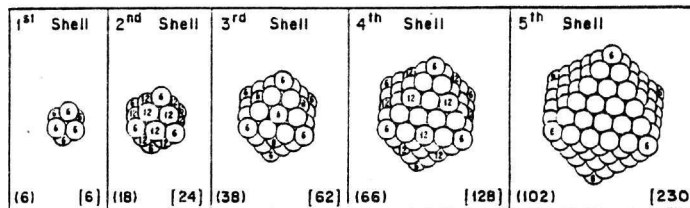
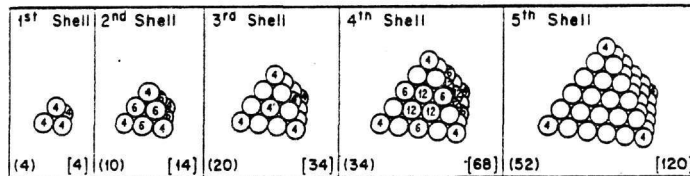
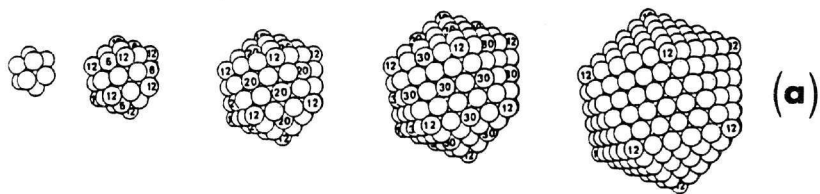
Fig.1. Mass spectra and related magic numbers of microclusters for (a) the rare gas xenon, (b) the semiconductor carbon, (c) the alkali-halide $[\text{Cs}(\text{CsI})_n]^+$ and (d) the alkali sodium.

similar information for carbon (Ross et al 1986), $[\text{Cs}(\text{CsI})_n]^+$ (Phillips 1986), and sodium clusters (knight et al 1984), respectively, is given. These are samples of rare gas, semiconductor, alkali-halide, and alkali microclusters, whose magic numbers are : $\eta = 1, 13, 55, 147, 309, 561, \dots; 4, 6, 10, 14, 18, \dots; 6, 14, 18, 20, 24, 30, 32, 38, 62, \dots;$ and $2, 8, 20, 40, 58, \dots,$ respectively.

In Figure 2(a)-(d) the geometrical explanation of the magic numbers appeared in Figure 1(a)-(d), respectively, is presented. Specifically, the magic numbers of rare gases are understood as closely packed nested icosahedral shells (Echt et al 1981, Anagnostatos 1987, 1988b), while those of semiconductors as nested tetrahedral shells (Anagnostatos 1990a), those of alkali halide (and of rare earths as well) as nested octahedral shells (Anagnostatos 1990c, 1991c), and those of alkali microclusters as nested equilibrium polyhedral shells as shown (Anagnostatos 1987). In all four cases the magic numbers result as the cumulative number of accommodated atoms from the beginning up to the point where a polyhedral shell is completed (or up to the point where a polyhedral shell is partially, symmetrically completed). At each block of all parts in Figure 2 (bottom left) the number of atoms accommodated by the relevant polyhedral shell is given and is utilized for the

estimation of magic numbers. For example, the second and third shell in Figure 2(a) accommodate 12 and 42 atoms, respectively, which lead to the major magic numbers $13=1+12$ and $55=13+42.$ Numbers written inside spheres of all parts in Figure 2 stand for the specific spheres (equal in number to the number shown) forming a partial, symmetric filling of the relevant polyhedral shell which (together with the spheres of all previous shells) give rise to a secondary magic number. For example, the numbers 6 and 12 inside spheres of the Figure 2(a) give rise to the secondary magic numbers $19=13+6$ and $25=13+12,$ where 13 is the previous magic number corresponding to the completion of the previous shell.

All details referring to the explanation of the magic numbers reported above can be found in the relevant cited references and thus there is no need of repeating them here in more extent than the previously given examples. At any rate, the important fact is not the demonstration of how the magic numbers result by proper summing up of complete polyhedral shells or subshells, but the very fact of demonstrating the specific symmetry supported in each case by the



(d)

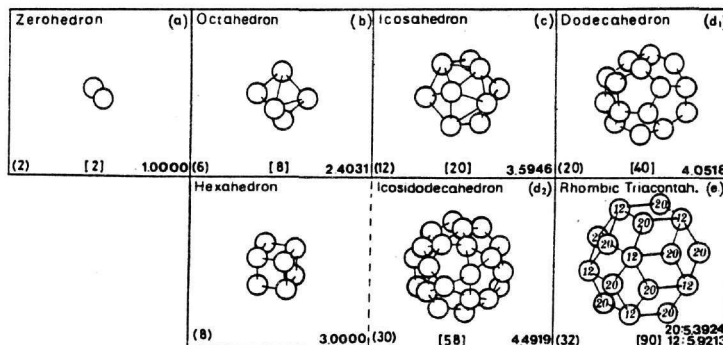


Fig.2. Geometrical explanation of magic numbers for the spectra shown in Figures 1(a)-(d). Specifically for (a) rare gases: close packing of spheres as nested icosahedral shells, (b) semiconductors: close packing of spheres as nested tetrahedral shells, (c) alkali-halides: close packing of spheres as nested octahedral shells, and (d) alkali homoclusters: close packing of shells as nested equilibrium polyhedral shells.

experimentally determined magic numbers and the implied similarities among them (Anagnostatos 1990b). Thus, the structure of rare gas microclusters is composed of concentric icosahedra, while that of semiconductors and alkali-halide microclusters is composed of concentric tetrahedra and concentric octahedra, respectively.

Despite the fact that each of the four structures in Figure 2(a)-(d) is made of geometrical shells, there is an important difference between Figures 2(a)-(c) and Figure 2(d). This difference is that in the first three structures we have close packing of spheres at the surface of each shell and overlapping between spheres of adjacent shells (soft spheres), while in the last structure we do not have close packing of spheres on each shell, but close packing of spheres (touching of spheres) between adjacent shells (hard spheres). By using the proper terminology, the first three cases correspond to close-packing of spheres, while the last case to close-packing of shells (Anagnostatos 1987). It is apparent that considering an effective atom-atom potential employed in the literature (e.g., Lennard-Jones potential), the close packing of spheres is energetically favored in comparison to the close packing of shells. However, if spheres presenting atoms are hard (as, for example, in alkali clusters), the corresponding structure can never follow the close-packing arrangement, since for such an arrangement an overlapping is inevitable which is prohibited for hard spheres. The physical property which makes an atom behave like a hard sphere will be discussed shortly.

For the explanation of magic numbers in alkali microclusters, besides the geometrical explanation given above (Figure 2(d)), an analytical approach has been employed in the literature as well (Knight et al 1984). In this approach all valence electrons of alkali atoms (i.e., one from each) are considered delocalized and under the influence of a central potential somehow created by the nuclear cores. This potential is given by Equation (1)

$$U(r) = - \frac{U_0}{\exp[(r-r_0)/\epsilon]} \quad (1)$$

where U_0 is the sum of the Fermi energy (3.23 eV) and the work function (2.7 eV) of the bulk; r_0 is the effective radius of the cluster sphere assumed to be $r_s N^{1/3}$, where r_s is the radius of a sphere containing one electron in the bulk ($r_s = 3.93$ a.u. for sodium, for example). The parameter ϵ

(=1.5 a.u.) determines the variation of the potential at the edge of the sphere. The Schrödinger equation is solved numerically for each N .

The level structure predicted by this potential is shown in Figure 3 together with the predicted magic numbers. It is very interesting for one to notice that in Figure 3 the numbers 18, 34, 64,... appear as magic numbers, while these numbers are not present either in the experimental mass spectrum of Figure 1(d) or in the interpretation of alkali magic numbers presented in Figure 2(d). This discrepancy between theory and experiments constitutes the starting point for a fundamental distinction between small clusters presented in Figure 1(a)-(c) and those in Figure 1(d). The former clusters are composed of atoms with an even number of electrons, while the latter ones are composed of atoms with an odd number of electrons. Thus, the first atoms could be seen as behaving like bosons and the last ones like fermions (Anagnostatos 1991b).

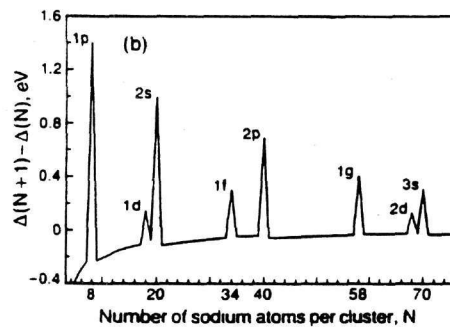


Fig.3. Electron level structure and magic numbers of alkali homoclusters, according to the jellium model(see Equation (1)).

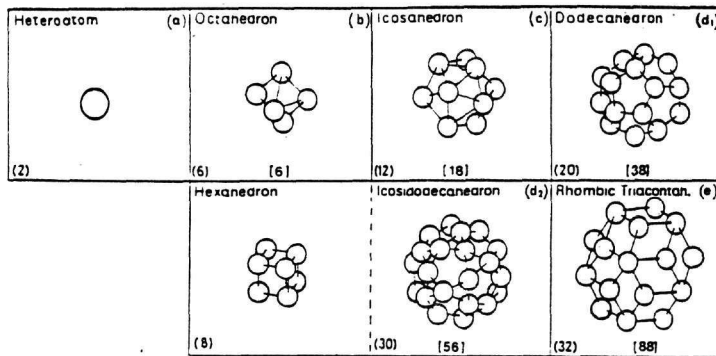
Furthermore, it is known that in the ground state, bosonic atoms (obeying the Boson statistics) try to occupy the lowest possible energy state, a fact which in geometrical language is consistent with the close packing of spheres (standing for atoms) as noted in Figures 2(a)-(c). Also as known, fermions (obeying the Fermi statistics) follow the Pauli principle forming shell structure and are never packed. Thus, Figure 2(d) is consistent with the fermionic nature of alkali atoms, where the polyhedra shown stand for shells of the alkali-atom average positions, or in other words these polyhedra represent the average motion pattern of the alkali atoms (Anagnostatos

1991a). Thus, the physics behind the soft-sphere like and hard-sphere like behavior of atoms in different microclusters is that the nature of particles is different for each of the two cases (i.e., bosonic and fermionic nature of atoms), a fact which makes their behavior like soft or hard spheres, or in other words permitting or not permitting overlapping between spheres of adjacent shells (Anagnostatos 1991b). More about the consequences of such a distinction between atoms will be reported below.

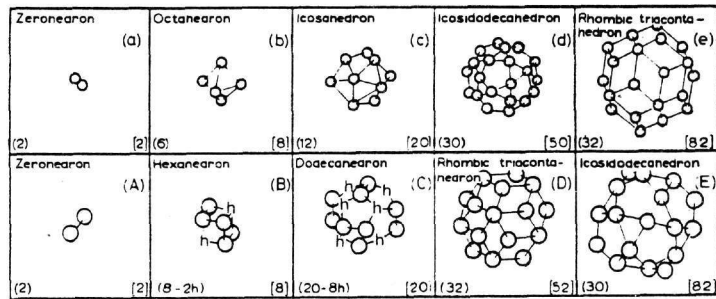
The distinction of atoms as bosons or fermions is consistent with the state of matter in the corresponding microclusters. Indeed, rare gas clusters (except He), for example, are considered solids, while alkali clusters are considered liquids (or gases) (Gspann 1986). Of course, this distinction of clusters according to the even or odd number of electrons in the atom is valid for born neutral atoms. For clusters born ionized (or very hot), however, we have conditions favoring delocalization of the valence electrons and thus the electron structure model (jellium model) of Figure 3 is valid, instead of the average structure of Figure 2(d) for the atoms in the cluster (Saito et al, 1988, 1989, Bhaskar et al 1987).

Now we can describe the conditions of validity between Figure 2(d) (due to atom structure) and Figure 3 (due to electron structure). The first is valid for alkali clusters born neutral, while the second for all other cases where a delocalization of valence electrons is favored. Indeed, in mass spectra of the second case the numbers 18, 34, 68 appear (Saito et al 1988, 1989), all of them being absent for neutral clusters as resulted from Figure 1(d) (Knight et al 1984).

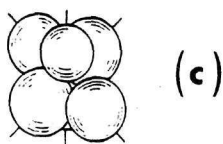
Figure 4(a)-(d) stands for the average structure of clusters involving neutral (fermionic) alkali atoms. Specifically, Figure 4(a) presents the average forms of shells for alkali-heteroatom (e.g., Mg) clusters (Anagnostatos 1989), while Figure 4(b) presents similar forms for clusters made up of two kinds of alkali atoms (e.g., K and Na) (Anagnostatos 1988a), Figure 4(c) presents the average form for a cluster made up of six alkali atoms each pair of which are of a different kind alkali (Anagnostatos 1991e), and finally Figure 4(d) presents a cluster of two alkali atoms, each of which is of a different kind. All about the magic numbers of Figures 4(a)-(b) coming from the geometry alone are shown on the figures themselves. The quantum mechanical analysis for



(a)



(b)



(c)



(d)

Fig.4. Average shell structure of microclusters involving neutral (fermionic) alkali atoms. Specifically for (a) alkali-heteroatom clusters, (b) two-component alkali clusters, (c) three-component alkali clusters, and (d) two-component alkali dimer.

clusters of Figures 4(a)-(b) is similar to the one given below for clusters of Figure 2(d) (Anagnostatos 1991a, 1991d). Semiclassical analysis for clusters of Figures 4(c)-(d) is similar to the one mentioned in the next section for the corresponding nucleon clusters.

It has been shown that quantum effects contribute to the mobility of the individual rare-gas atoms in microclusters (starting from the zero-point kinetic energy) and to the superposition of different configurations in the same clusters, as explained in Franke et. al. (1988). Here we deal with the quantum mechanics of the neutral alkali atoms (taken as fermions, as already has been discussed above) which form shells in microclusters. We further assume that all alkali atoms of a shell taken together create an average central potential common for all atoms in that shell. In this potential each atom is considered as performing an independent particle motion (like nucleons in nuclei) obeying the Schrödinger equation for this potential. Further, our analysis proceeds by considering a multi-harmonic oscillator potential as follows (Anagnostatos 1990a, 1991d).

$$H = H_{1s} + H_{1p} + H_{1d2s} + \dots \quad (2)$$

$$\text{where } H_i = V_i + T_i = -V + 1/2 m(\omega_i)^2 r^2 + T_i \quad (3)$$

That is, we consider a state-dependent Hamiltonian, where each partial harmonic oscillator potential has its own state-dependent frequency ω_i . All these ω_i 's are determined from the harmonic oscillator relation (Hornyak 1975).

$$\hbar\omega_i = (\hbar^2/m \langle r_i^2 \rangle)^{1/2} (n_i + 3/2), \quad (4)$$

where n_i is the harmonic oscillator quantum number and $\langle r_i^2 \rangle^{1/2}$ is the average radius of the relevant high fluxional shell from Figure 2(d).

The solution of the Schrödinger equation with Hamiltonian (2), in spherical coordinates, is

$$\Psi_{nlm}(r, \theta, \varphi) = R_{nl}(r) Y_l^m(\theta, \varphi), \quad (5)$$

where $Y_l^m(\theta, \varphi)$ are the familiar spherical harmonics and the expressions for the $R_{nl}(r)$ are given in several books of Quantum Mechanics and Nuclear Physics, for example see Table 4-1 of Hornyak (1975). The only difference between our wave functions and those in these books is

the different ω 's as stated in (2)-(4) above. Those of our wave functions, however, which have equal ℓ value, because of the different $\hbar\omega$, are not orthogonal, since in these cases the orthogonality of Legendre polynomials does not suffice. Orthogonality, of course, can be obtained by applying established procedures, e.g., Gram-Schmidt process.

According to the Hamiltonian of (2), the binding energy of a cluster with N atoms in the case of orthogonal wave functions takes the simple form given by (6)

$$BE = 1/2 (V \cdot N) - 3/4 \left[\sum_{l=1}^N \hbar\omega_l (n_l + 3/2) \right], \quad (6)$$

where V is the average potential depth discussed further shortly. The coefficients $1/2$ and $3/4$ take care of the double counting of atom pairs in determining the potential energy.

The average depth of the potential in its general case and in analogy to nuclei, is given by (7)

$$V = aN + b, \quad (7)$$

where if $a=0$ the potential has a fixed depth for all values of N . Specifically for completed polyhedra, an extra term is taken, i.e.

$$V = (-aN + b) + c/N. \quad (8)$$

This term expresses the energetic advantage for a microcluster to have a spherical (compact) structure, i.e., according to Figure 2(d), to have completed all polyhedral shells involved in that structure. This coefficient c expresses the sphericity of the cluster and has the same numerical value everytime the outermost polyhedron of the structure is completed. Everywhere else c has a zero value.

Following Chou et al (1984) the relative binding energy change for a cluster with N atoms compared to clusters with $N + 1$ and $N - 1$ atoms is given by (9).

$$\begin{aligned} \delta(N) &= [E_B(N) - E_B(N-1)] - [E_B(N+1) - E_B(N)] = \\ &= 2 E_B(N) - [E_B(N-1) + E_B(N+1)]. \end{aligned} \quad (9)$$

The point-atom root mean square (rms) radius of a neutral alkali microcluster containing N

atoms is determined by employing our wave functions, as shown in (10).

$$\langle r^2 \rangle^{1/2} = \left(\sum_{i=1}^N \langle r_i^2 \rangle / N \right)^{1/2}, \quad (10)$$

where the individual $\langle r_i^2 \rangle^{1/2}$ values come from Figure 2(d). These radial sizes of the polyhedra in Figure 2(d) are determined by employing (11).

$$R_x = \langle r^2 \rangle_{\text{shell}}^{1/2} = R \cos \alpha + (4R_0^2 - R^2 \sin^2 \alpha)^{1/2}, \quad (11)$$

where R_x is the radius of the polyhedron to be determined, R the radius of the previous polyhedron in contact, R_0 the radius of the sphere standing for an alkali atom, and α the angle defined by the symmetry and relative orientation of both shells involved according to Coxeter (1973). The values of R_x so derived are given in Figure 2(d) in units R_0 at the right-bottom corner of each block.

In Figure 5 the relative binding energy $\delta(N)$ versus N is plotted for the parameter values (see (8)) $a = 0.2$ and $c = 1.0 (\hbar^2 / (mR_0^2))$. Discontinuities are observed precisely at the magic numbers. Even more, the relative sizes of the discontinuities (except perhaps at $N=90$) resemble those observed in the abundance curve during the cluster formation.

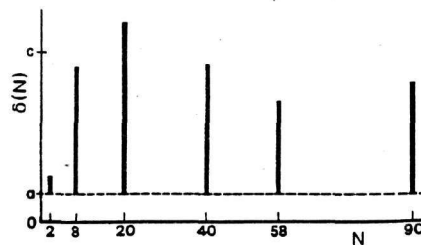


Fig. 5. Relative binding energy, $\delta(N)$, versus size, N , of alkali homoclusters. See Equations (9) and (10) for $a=0.2$ and $c=1.0 (\hbar^2 / (mR_0^2))$.

Odd-even staggering (Bjornholm et al 1990) in mass spectra of alkali clusters is evidence that attractive forces, e.g. forces between atoms, play an important role in the cluster stability. Also, the observed cluster deformation (Lipparini et al 1989) between closed shells points again to the importance of equilibrium geometry of atoms. Thus, odd-even staggering and

deformation effects support the present model, as ionization potential and polarization measurements (Knight et al 1984, Kappes 1988) support the jellium model.

The jellium model and the present model are applicable to microclusters of the same elements (alkali or alkali-like) but for different conditions which favor or do not favor electron delocalization.

All discussion specified here for alkali atoms is obviously also valid and experimentally supported (Pettiette et al 1988, Katakuse and Ichihara 1986) for alkali-like atoms, i.e., for Cu, Ag, Au.

Besides the novel quantum mechanical explanation of magic numbers for neutral alkali (or alkali-like) atoms, the present work underlines the idea that new, yet unobserved properties of neutral alkali microclusters should be investigated. Perhaps, the most important of them are the orbiting properties of atoms implying a series of properties due to orbital angular momentum, i.e., definite spin properties, independent particle and collective modes of excitation of individual species, etc. For an experimental verification of such properties nuclear methods should be employed.

3. NUCLEON (QUANTUM) CLUSTERS

Neutrons and protons are fermions and according to the most recent advances of particle physics are not point particles but particles with finite sizes as presented by the sizes of their bags (e.g., 0.8-1.1 fm according to Thomas 1984). In this respect nuclear structure could be seen as similar to neutral-alkali cluster structure with the main differences being:

- (i) the different sizes of spheres representing the nucleons and the alkali atoms and
- (ii) the different strength and other details of the relevant state dependent potential (see Equation 3).

However, Figure 4(b) is valid for the average forms of both neutral alkali clusters and nucleon clusters. It is satisfying that both kinds of clusters exhibit the same set of magic numbers (see

numbers in brackets in Figure 4(b)). The geometry of the equilibrium polyhedra of this figure is not a fixed geometry like the one we are familiar with in solid state physics, but it is simply a geometrical representation of high fluximal shells like those we are familiar with from the molecular orbitals.

Besides Figure 4(b), Figure 4(c) and (d) presents average structures valid for both neutral alkali clusters and nucleon clusters. Specifically, Figure 4(c) shows the average structure of clusters consisting of three kinds of neutral alkali atoms (two atoms for each kind, e.g., Li, K, and Na) (Anagnostatos 1991e), while for nucleon clusters it presents the average structure of $^6_{\Lambda\Lambda}\text{He}$ (i.e., of two neutrons, of two protons, and of two Λ hyperons; Anagnostatos and Grypeos 1990). Figure 4(d) for atomic clusters presents a snapshot of the simplest mixed alkali clusters (e.g., K and Na), while for nucleon clusters presents a similar snapshot for the deuteron (e.g., one n and one p) (Anagnostatos et al 1990). Details for both alkali and nucleon clusters can be found in the cited references.

4. CONCLUDING REMARKS

The properties of small clusters substantially differ from the properties of the same material in bulk. The present study is centered around a characteristic property of small clusters called magic numbers whose significance in the structure of clusters is similar to that of magic numbers in nuclear structure.

The magic numbers in small clusters are different for the different groups of elements (homo-clusters) or the different mixtures of these groups (hetero-clusters).

Elements with an even number of electrons behave like bosons in cluster structure, while elements with an odd number of electrons behave like fermions (Anagnostatos 1991b). The structure of bosonic clusters is closely approximated by packing of spheres arrangements possessing specific symmetry characteristic to the specific element comprising the cluster (e.g., rare gas clusters exhibit nested icosahedral structure as shown in Figure 2(a), while

semiconductor clusters exhibit nested tetrahedral structure as shown in Figure 2(b)). The structure of fermionic clusters (only their average structure) can be presented by packing of equilibrium-polyhedral shell arrangement common for all relevant groups of elements and obeys the Pauli principle. (see Figures 2(d) and 4).

Clusters discussed here are composed of neutral atoms. Such clusters have been born neutral and the ionization used later to facilitate their detection does not, usually, alter their structure. However, clusters born ionized favor delocalization of the valence electrons. All such electrons in the cluster are assumed in a central potential which is responsible for the appearance of the relevant magic numbers due to electron structure. This central potential, however, is created by the spherical packing of the atomic ion cores (i.e., of atoms without valence electrons), a fact which is responsible for the appearance of additional magic numbers due to atoms like in bosonic clusters. Besides the method of cluster production, other facts favoring delocalization of valence electrons are the cluster temperature, the cluster size, etc.

It is of great interest that fermionic atomic clusters exhibit magic numbers similar to those in nuclei (composed, also of fermions). This very fact gives a hint for an alternative study of nuclei resembling the study of fermionic atomic clusters and vice versa (Anagnostatos 1985). In this case, for example, the diatomic alkali cluster KNa could be studied in a parallel way like the deuteron (Anagnostatos et al 1990). More applications of this alternative study of nuclei will appear elsewhere.

Finally, one could remark that both small clusters and finite nuclei are cases of aggregates with a small number of particles and because of this we have all similarities described briefly above. In the cases where the number of particles becomes infinite the small cluster structure approaches crystal structure, while nuclear structure approaches nuclear-matter structure. Both systems of aggregates (small clusters and nuclei) could be seen as matter in small volumes and could be treated as fifth state of matter.

REFERENCES

Anagnostatos G.S. 1985 Int. J. Theor. Phys. **24**, 579

Anagnostatos G.S. 1987 Phys. Lett. A **124**, 85

Anagnostatos G.S. 1988a Phys. Lett. A **128**, 266

Anagnostatos G.S. 1988b Phys. Lett. A **133**, 419

Anagnostatos G.S. 1989 Phys. Lett. A **142**, 146

Anagnostatos G.S. 1990a Phys. Lett. A **143**, 332

Anagnostatos G.S. 1990b Phys. Lett. A **148**, 291

Anagnostatos G.S. 1990c Phys. Lett. A **150**, 303

Anagnostatos G.S. 1991a Phys. Lett. A accepted for publication

Anagnostatos G.S. 1991b Phys. Lett. A to appear

Anagnostatos G.S. 1991c Phys. Lett. A to appear

Anagnostatos G.S. 1991d Z. Phys. D accepted for publication

Anagnostatos G.S. 1991e Z. Phys. D accepted for publication

Anagnostatos G.S., Grypeos M.E. , 1990 Proceedings of the PANIC XII International Conference on Particles and Nuclei, Cambridge (MIT), p. IV-25.

Anagnostatos G.S., Gridnev K.A., Subbotin V.B. 1990. Proceedings of the "ISSPIC5 5th International symposium on Small Particles and Inorganic Clusters", Konstanz, p. MO81.

Bhaskar N.D., Frueholz R.P., Klimcak C.M. and Cook R.A. 1987, Phys. Rev. B **36**, 4418.

Bjorholm S., Borggreen J., Echt O., Hansen K., Rasmussen H.D. and Pedersen J 1990 Proc. of the "5th International Symposium on Small Particles and Inorganic Clusters" ISSPIC5, Konstanz, September 10-14, p. M076.

Chou M.Y., Cleland A., Cohen M.L. 1984, Solid State Comm. **52** 645.

Coxeter H.S.M. 1973 Regular Polytopes (New York: Macmillan).

Echt O., Sattle K. and Recknagel E 1981, Phys. Rev. Lett. **47**, 1121.

Franke G., Hilf E. and Palley L. 1988, Z. Phys. D **9** 343.

Gspann G. 1986, Z. Phys. D **3**, 143.

Hornyak W.F. 1975 Nuclear Structure (New York: Academic) pp 252, 238, 240, 235.

Kappes M.M. 1988 Chem. Rev. **88** 369.

Katakuse I., Ichihara T. 1986, Int. J. Mass Spectr. Ion Proc. **74**, 33.

Knight W.D., Clemenger K., de Heer W.A., Saunders W.A., Chow M.Y. and Cohen M.L. 1984
Phys. Lett. **52**, 2141.

Lipparini E., Stringari S. 1989 Phys. Rev. Lett. **63**, 570.

Pettiette C.L., Yang S.H., Craycraft M.J., Conceicao J., Laaksonen R.T., Cheshnovsky O. and
Smalley R.E. 1988. J. Chem. Phys. **88**, 5377.

Phillips J.C., 1986 in Proceedings of the International Symposium on the Physics and
Chemistry of Small Clusters eds Jena P, Rao B.K. and Khanna S.N., Richmond p. 249.

Ross M.M., O'Keefe A., and Baronavski A.P. 1986 in Proceedings of the International
Symposium on the Physics and Chemistry of Small Clusters eds Jena P, Rao B.K. and
Khanna S.N., Richmond p. 323.

Saito Y., Watanabe M., Hagiwara T., Nishigaki S. and Noda T., 1988 J. Appl. Phys. **27** 424.

Saito Y., Minami K., Ishida T. and Noda T. 1989, Z. Phys. D **11** 87.

Thomas A.W. 1984 in Adv. Nucl. Phys. eds Negele J.W. and Vogt E. **13**, 1.